IEEE Journal of Translational Engineering in Health and Medicine

Received 12 May 2014; revised 11 July 2014; accepted 16 August 2014. Date of publication 4 September 2014; date of current version 12 September 2014.

Digital Object Identifier 10.1109/JTEHM.2014.2354332

Pre to Intraoperative Data Fusion Framework for Multimodal Characterization of Myocardial Scar Tissue

ANTONIO R. PORRAS[1], GEMMA PIELLA[1], ANTONIO BERRUEZO[2], JUAN FERNÁNDEZ-ARMENTA[2], AND ALEJANDRO F. FRANGI[3], (Fellow, IEEE)

[1]Center for Computational Imaging and Simulation Technologies in Biomedicine, Department of Information and Communication Technologies, Universitat Pompeu Fabra, Barcelona 08002, Spain

[2]Hospital Clínic de Barcelona, Institut d'Investigacions Biomèdiques August Pi i Sunyer, Universitat de Barcelona, Barcelona 08036, Spain

[3]Center for Computational Imaging and Simulation Technologies in Biomedicine, Department of Mechanical Engineering, University of Sheffield, Sheffield S10 2TN, U.K.

CORRESPONDING AUTHOR: A. R. PORRAS (antonio.porras@upf.edu)

This work was supported by the Spanish Ministry of Economy and Competitiveness under Grant TIN2009-14536-C02 and Grant TIN2012-35874. The work of A. R. Porras was supported by the Spanish Government within a Formación del Profesorado Universitario Grant.

ABSTRACT Merging multimodal information about myocardial scar tissue can help electrophysiologists to find the most appropriate target during catheter ablation of ventricular arrhythmias. A framework is presented to analyze and combine information from delayed enhancement magnetic resonance imaging (DE-MRI) and electro-anatomical mapping data. Using this information, electrical, mechanical, and image-based characterization of the myocardium are performed. The presented framework allows the left ventricle to be segmented by DE-MRI and the scar to be characterized prior to the intervention based on image information. It allows the electro-anatomical maps obtained during the intervention from a navigation system to be merged together with the anatomy and scar information extracted from DE-MRI. It also allows for the estimation of endocardial motion and deformation to assess cardiac mechanics. Therefore, electrical, mechanical, and image-based characterization of the myocardium can be performed. The feasibility of this approach was demonstrated on three patients with ventricular tachycardia associated to ischemic cardiomyopathy by integrating images from DE-MRI and electro-anatomical maps data in a common framework for intraoperative myocardial tissue characterization. The proposed framework has the potential to guide and monitor delivery of radio frequency ablation of ventricular tachycardia. It is also helpful for research purposes, facilitating the study of the relationship between electrical and mechanical properties of the tissue, as well as with tissue viability from DE-MRI.

INDEX TERMS Arrhythmia, catheter ablation, DE-MRI, electro-anatomical mapping system, ventricular tachycardia.

I. INTRODUCTION

Catheter ablation is a procedure used to treat some types of arrhythmia, when drug therapies are not effective. One type of arrhythmia that is usually treated with this procedure is Ventricular Tachycardia (VT) associated with Ischemic Cardiomyopathy (IC).

After a myocardial infarction, myocardial cells die because of the lack of oxygen supply, creating fibrotic areas where electrical impulses are not propagated. Around and through these areas of dense fibrosis, other areas with low-density fibrosis where the impulse is propagated with a low velocity appear. Sometimes, these areas of slow conduction represent corridors with at least two connections with healthy muscle, being the substrate for reentrant VTs. These slow conduction corridors or conducting channels are the target for VT ablation [1], [2].

Different information sources have been used during the last years to identify the conducting channels that are responsible for reentrant VTs. Delayed Enhancement Magnetic Resonance Imaging (DE-MRI) is used to find the ablation

target prior to the intervention, while Electro-Anatomical Mapping (EAM) systems are used intra-operatively. In clinical practice, these two information sources are used separately to characterize cardiac tissue based on different properties. In this paper, a new framework that allows the integration of images from DE-MRI, electrical measurements and mechanical properties estimated using an EAM system is presented.

II. BACKGROUND

Recently, many approaches have been developed to characterize scar tissue from different information sources. In this section, a short review of methods for scar characterization from DE-MRI, electrical and mechanical information obtained from EAM systems is presented.

A. PRE-OPERATIVE SCAR CHARACTERIZATION

DE-MRI has become the standard modality to localize and quantify areas of scar, viable and healthy myocardial tissue pre-operatively [3]–[5]. The acquired images visualize the uptake of a contrast agent by the intracellular space after a given time from the administration of the contrast. Healthy myocardium and scar tissue have different uptake profiles and hence, are imaged differently (fibrotic areas appear brighter than healthy myocardium). DE-MRI could be used for ablation planning by identifying pre-operatively the target ablation areas during the procedure [6]–[9]. However, the inherent limitations of MRI leading to imaging artifacts can lead to errors when identifying scar tissue [6], [10]. In addition, the spatial resolution limits the detection of the border zone channels in the dense scar tissue, since these channels can be very narrow [8], [11].

Different segmentation methods from DE-MRI have been proposed during recent years [12]–[14]. Having the segmentation of the myocardium, the scar can be localized based on voxel intensities, since it appears significantly brighter than healthy myocardium. To recover the anatomical structure of the scar automatically, threshold-based methods have been proposed [3], [15]. Other approaches imposing geometrical constraints have been presented to improve the consistency of the results [16], [17]. Cluster-based and support vector machine methods have also been proposed [12], [18], [19].

B. INTRA-OPERATIVE ELECTRICAL CHARACTERIZATION

Different EAM systems have been developed during recent years to guide catheter ablation. One such system is Carto (Biosense Webster, Haifa, Israel). It uses magnetic fields to track the position and orientation of the catheter. When the catheter is properly positioned, it allows the electrical activity at its tip to be recorded; then, based on the tracked position of the catheter tip, the system shows a spatial reconstruction of the mapped cavity, also providing the electrical signals recorded. It is also possible to use an additional software module that allows pre-operative images to be integrated for a better visualization and interpretation of the acquired information.

During the intervention, it is necessary to accurately locate and characterize the scar tissue to find the conducting channels responsible for the VT, which are the ablation target. Mapping during stable rhythm allows the characterization of the arrhythmogenic substrate. After the acquisition, different electrical parameters are used to identify the ablation target, such as the maximum bipolar and unipolar voltages, and the local activation time. Scar core, border zone and healthy tissue can be classified using voltage thresholds. However, there are no standard thresholds that can be used for all patients [20], which makes the cardiologist's expertise a key factor in a successful intervention. In addition, data obtained from EAM systems have several limitations for a precise characterization of the arrhythmogenic substrate (i.e. far-field effect, time-consuming, poor tissue contact).

C. INTRA-OPERATIVE MECHANICAL CHARACTERIZATION FROM EAM DATA

Other types of information, such as myocardial mechanics, can also be considered to better characterize the scar [21] and, therefore, to improve the result of the ablation procedure. It is possible to assess cardiac mechanics during the intervention by using catheter tracking information to estimate cardiac contractility [22], [23]. NOGA (Biologics Delivery Systems Group, Cordis Corporation, Irwindale CA, USA) was developed to estimate cardiac mechanics for tissue viability assessment. A technique to integrate electrical and motion information was described in [24] as part of this system and different clinical applications were proposed in [21]. In [22], a methodology to estimate 3D endocardial motion and deformation fields from electro-anatomical data and a pre-operative image was proposed.

The limitations of the aforementioned methods are related to the accuracy of the catheter tracking system and the presence of components in the recorded motion signals that are not directly related to cardiac motion (i.e. motion related to respiration [22]).

D. INTEGRATION OF MULTI-MODAL INFORMATION

Even though scar tissue can be characterized from different information sources, all of them have some limitations. In addition, the results obtained from different sources are based on different tissue properties, so the shape and extent of the scar identified using each modality is not necessarily the same [7], [20], [25].

The information from the different sources could be considered together for a better characterization of myocardial tissue. In [7] and [11], a correlation between the conducting channels inside the scar detected by DE-MRI and EAM systems was found. In [26], it was shown that integrating electrical and mechanical information provided better results than using each type of information separately. However, to the best of our knowledge, there are no known tools that allow the integration of the information from DE-MRI with electrical and mechanical properties of the heart. In this paper, a framework is presented where these three sources of

IEEE Journal of Translational Engineering in Health and Medicine

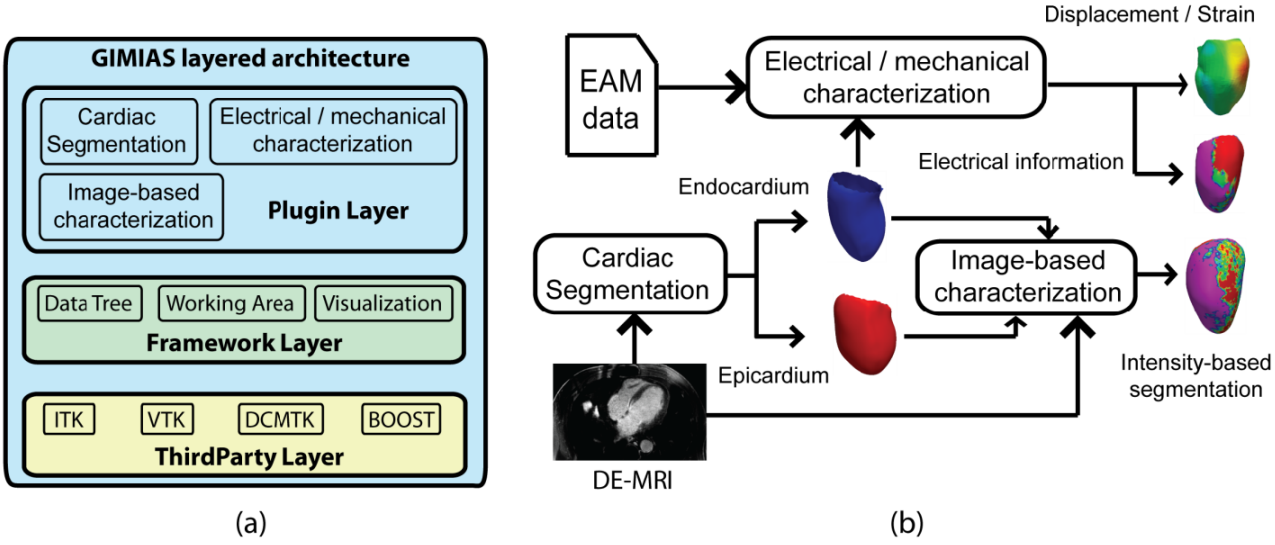

FIGURE 1. **(a) Layered architecture of GIMIAS. The Plugin layer is on the top and plugins can interoperate through the elements at the framework layer. The Third Party layer is at the bottom, to which all modules have access. (b) Presented pipeline. Both endocardium and epicardium meshes are segmented from DE-MRI using the cardiac segmentation module. The output meshes are used by the image-based characterization module to characterize the scar based on voxel intensities. The segmented endocardium is also used, together with electro-anatomical mapping data, for electrical and mechanical characterization of the left ventricle.**

information are integrated for multimodal left-ventricular myocardial tissue characterization.

III. METHODS AND PROCEDURES

The presented framework has a modular design, integrating three different modules to support the process of scar characterization: cardiac segmentation, image-based characterization and electrical/mechanical characterization from the data recorded with an EAM system. These modules were integrated in GIMIAS (www.gimias.org) [27], which is a workflow-oriented open-source environment that can be extended through the development of problem-specific plug-ins. The implementation was done in the C++ language.

The layered architecture of GIMIAS is represented in Fig. 1(a). Each of the modules for scar characterization is located at the Plugin Layer and can be used independently of the others. Meshes, images, signals or any type of information are attached to the main data tree and are directly accessible by any other module. Fig. 1 (b) shows a schematic describing how the presented modules inter-operate. In the following sections, each of the modules for scar characterization will be presented.

A. CARDIAC SEGMENTATION

The cardiac segmentation module provides algorithms for a semi-automatic segmentation of 3D+t images of the heart from different modalities. The underlying methodology is the same for all modalities, which brings a great advantage when integrating multiple sources of image data.

The method uses a deformable model that encodes statistical information about the shape of the heart based on a Point Distribution Model (PDM). The PDM was built from 134 patients in 15 cardiac phases, totaling 2010 training volumes [28], [29]. The segmentation algorithm has been trained and evaluated on CT [28], SPECT [30], 3D US [31] and MRI [32] datasets.

To segment the left ventricle, the user sets three landmarks in the images: one at the center of the aortic valve, one at the center of the mitral valve and another one at the apex. The software positions and scales the average shape in the PDM based on these three landmarks. This PDM contains both the endocardium and the epicardium, and acts as a template that is adapted to the geometry of each patient's heart [33]. Manual corrections can be performed to fix possible errors in the results from the automatic processing. These corrections can be applied either freely or by imposing statistical constraints.

B. IMAGE-BASED CHARACTERIZATION

The second module in the pipeline was designed for scar characterization from DE-MRI. It needs the model of the left ventricle to be segmented using the cardiac segmentation module as an input. This module divides the segmented ventricle into a number of layers that can be selected by the user from the endocardium to the epicardium, obtaining a 3D shell for each of the layers. One signal intensity map at each layer is obtained by summing the intensity of all the voxels between neighboring layers, as explained in [8]. This information is then projected onto each shell.

Scar areas can be differentiated from healthy myocardium based on the distribution of the intensities in the image, since scar tissue appears brighter in DE-MRI. Moreover, scar core and border zone can also be identified using thresholds, as previously reported in [7]. Based on this study, areas with

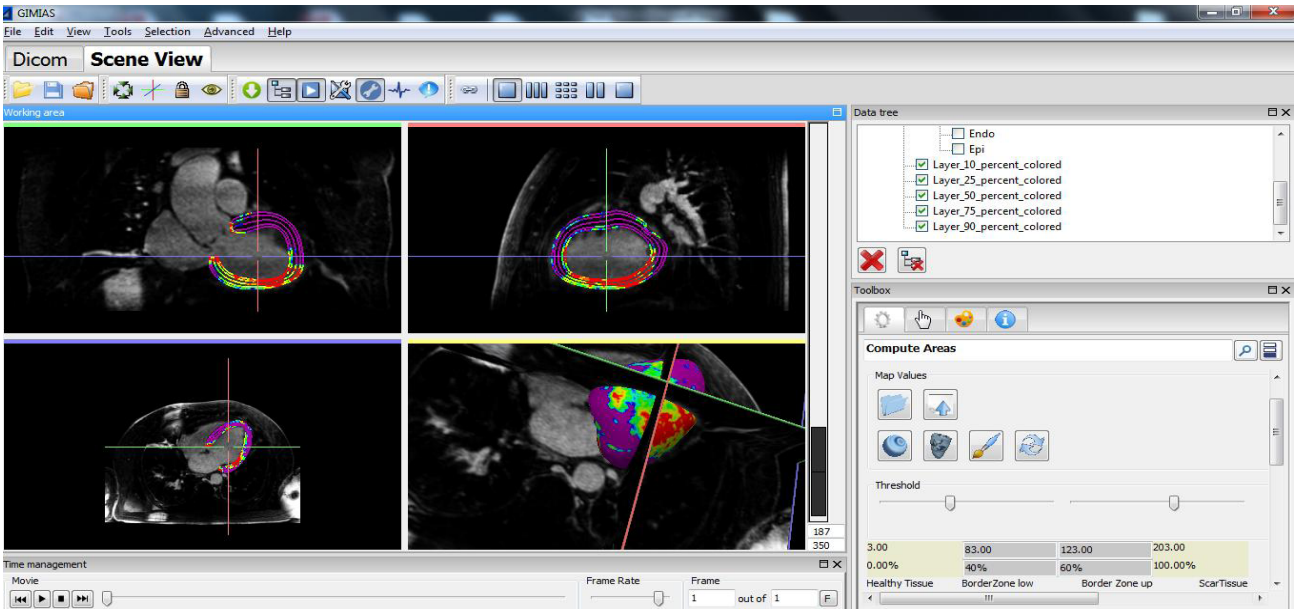

FIGURE 2. **Layers extracted from the left ventricle model segmented with the cardiac segmentation module. Tissue classification based on image intensities is color coded. Red represents dense scar tissue, green represents viable tissue (border zone) and purple represents healthy myocardium.**

signal intensities higher than 60% of the maximum are classified as scar core, while areas with signal intensities lower than 40% of the maximum are classified as healthy tissue. The remainder of the tissue is considered as border zone. However, since image artifacts may affect the intensity range in the image, these thresholds may need to be adjusted manually. Finally, this threshold-based classification can be visualized in 3D through color-coded maps in every transmural shell. Fig. 2 shows one example of segmentation of a left ventricle with scar tissue characterized based on image intensity levels using the presented framework.

C. ELECTRICAL/MECHANICAL CHARACTERIZATION

The third module in the pipeline allows both electrical and mechanical characterization of the tissue using EAM data and a left ventricle model segmented using the cardiac segmentation module. In particular, electro-anatomical maps imported from the Carto system are used.

This module allows electro-anatomical data to be loaded and used intra-operatively in a catheter-guided intervention. It is possible to visualize all the electrical signals recorded, together with the catheter tracking information. The maximum bipolar voltage, maximum unipolar voltage and local activation time at each point are calculated for electrical characterization of the tissue. The trajectory of the catheter (which is in contact with the endocardium) during the acquisition of the local electrograms can also be visualized (see Fig. 3).

The cloud of points acquired during the intervention can be registered to the endocardial surface extracted from the cardiac segmentation module. This is done by selecting at least three landmarks in both the surface and the cloud of points. Then, an Iterative Closest Point (ICP) algorithm [34] can be used to improve the registration results. If ventricle segmentation is used intra-operatively to guide the intervention, it is also possible to load the transformation matrix calculated intra-operatively, getting the same registration used during the intervention. After registration, all the electrical parameters on the endocardial surface can be projected and interpolated. They can also be projected into any of the different layers with scar information obtained from DE-MRI, allowing the visualization of the information from both sources on the same surface.

Once the ventricle shape and the points from the EAM system are registered, it is also possible to estimate endocardial motion and deformation using the method presented in [22]. This method extracts the catheter trajectories during one cardiac cycle and synchronizes the motion signals of all the points acquired. Then, catheter trajectories are projected into the endocardial mesh using a bilinear atlas to help interpolate motion in the areas where this information is not available. The result is a 3D+t endocardial mesh where both displacement field and directional strains are also calculated, providing mechanical information at each time point.

Finally, all the information can be visualized into the 17-segments model proposed by the American Heart Association (AHA) [35]. Curves showing the evolution of displacement and strain can also be obtained and exported. As an illustration, Fig. 3 shows a cloud of EAM points registered to a left ventricle segmentation, together with the electrical scar characterization.

D. DE-MRI ACQUISITION PROTOCOL

All patients included in the study underwent a DE-MRI exam prior to the ablation procedure (median 2 days, interquartile

IEEE Journal of Translational Engineering in Health and Medicine

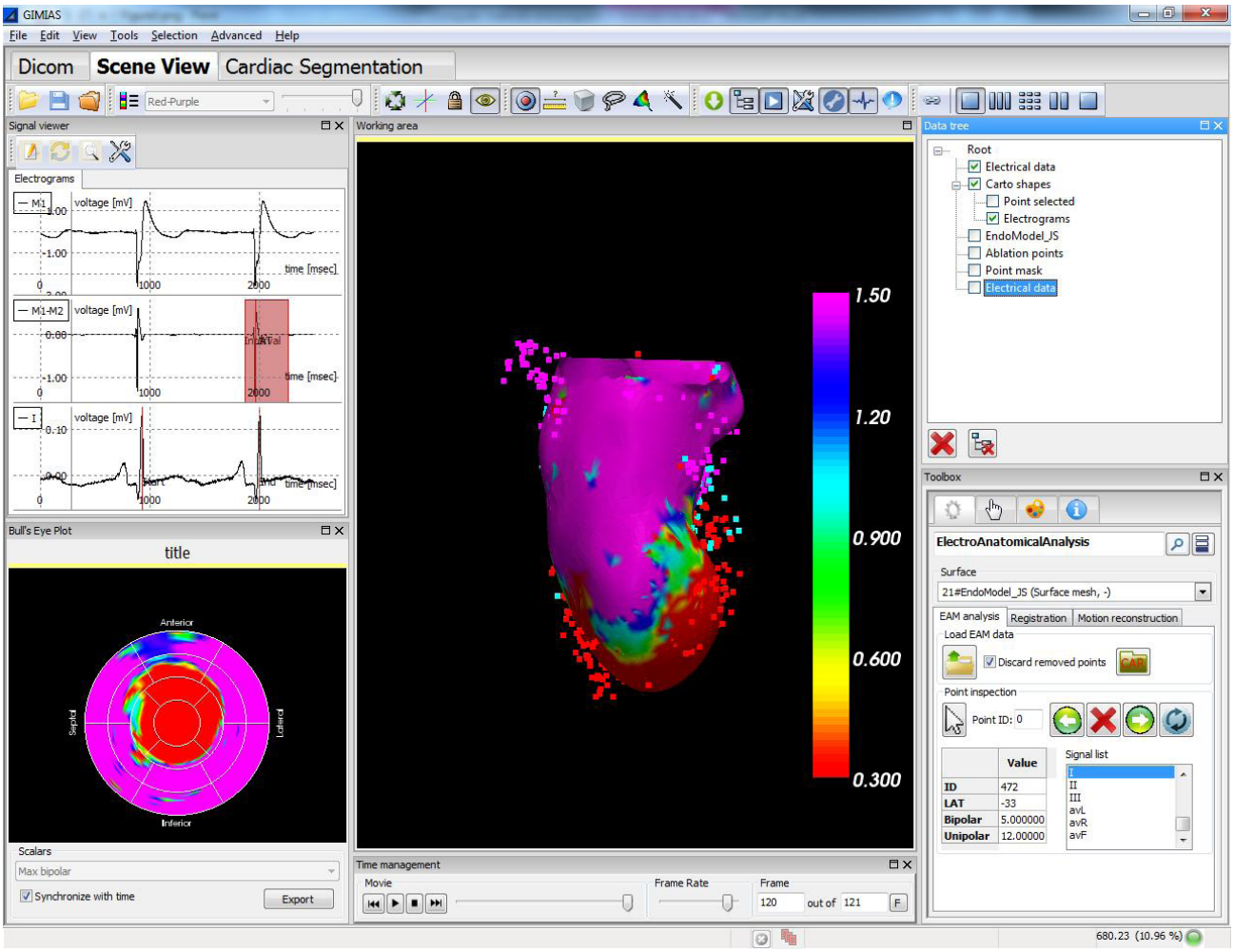

FIGURE 3. **Electrical characterization of the tissue. EAM points are registered to the left ventricle endocardium. Electrical parameters derived from the recorded electrograms are interpolated on the mesh. The image shows the maximum bipolar voltage color coded. Purple color represents healthy tissue (>1.5mV) and red color represents dense scar (<0.5mV). The information is also represented using the 17-segments model proposed by the American Heart Association. Bipolar, unipolar electrograms and superficial ECG (lead I) are also shown in the upper left corner for one selected point.**

range 1–6 days). A 3-Tesla scanner (Magnetom Trio, Siemens Medical Solutions, Erlangen, Germany) equipped with advanced cardiac-dedicated software and a cardiac 12-element phased array coil was used. Patients were instructed to maintain shallow breathing during the acquisition. Seven minutes after intravenous administration of gadodiamide-DTPA (Omniscan, Amersham Health) at a dose of 0.2 mmol/kg, a whole-heart, high spatial resolution, DE-MRI study was conducted using a free-breathing, navigator-gated, 3D inversion-recovery, gradient echo technique [36]. The 3D slab was acquired in the transaxial direction. Slice thickness was 1.4 mm, with no gap between slices. The field of view (FOV) was set to 360 mm and matrix size was kept at 256 × 256 pixels to yield an isotropic spatial resolution of 1.4 × 1.4 × 1.4 mm. Image acquisition was ECG-gated to end-diastole to minimize cardiac motion. A standard delayed-enhanced dataset was obtained by applying a 2D IR-TurboFLASH sequence in sequential 5 mm slices with no gap between them, to cover both ventricles in the short-axis orientation in addition to the 2-, 3-, and 4-chamber views.

E. ELECTROPHYSIOLOGY AND SUBSTRATE MAPPING

The electrophysiology study was performed under conscious sedation. A tetrapolar diagnostic catheter was positioned at the right ventricular apex. Trans-septal or retro-aortic approaches were used for left ventricular access. An endocardial high-density 3D electro-anatomical bipolar voltage map of the left ventricle was obtained during stable sinus rhythm using the Carto system. Standard voltage thresholds (<0.5 mV for the core and <1.5 mV for the border zone) were used to define the scar on the EAM. The conducting channels on the EAM were visually identified as: (i) corridors of border zone (maximum bipolar voltage between 0.5 and 1.5 mV) within scar core areas or between a scar core

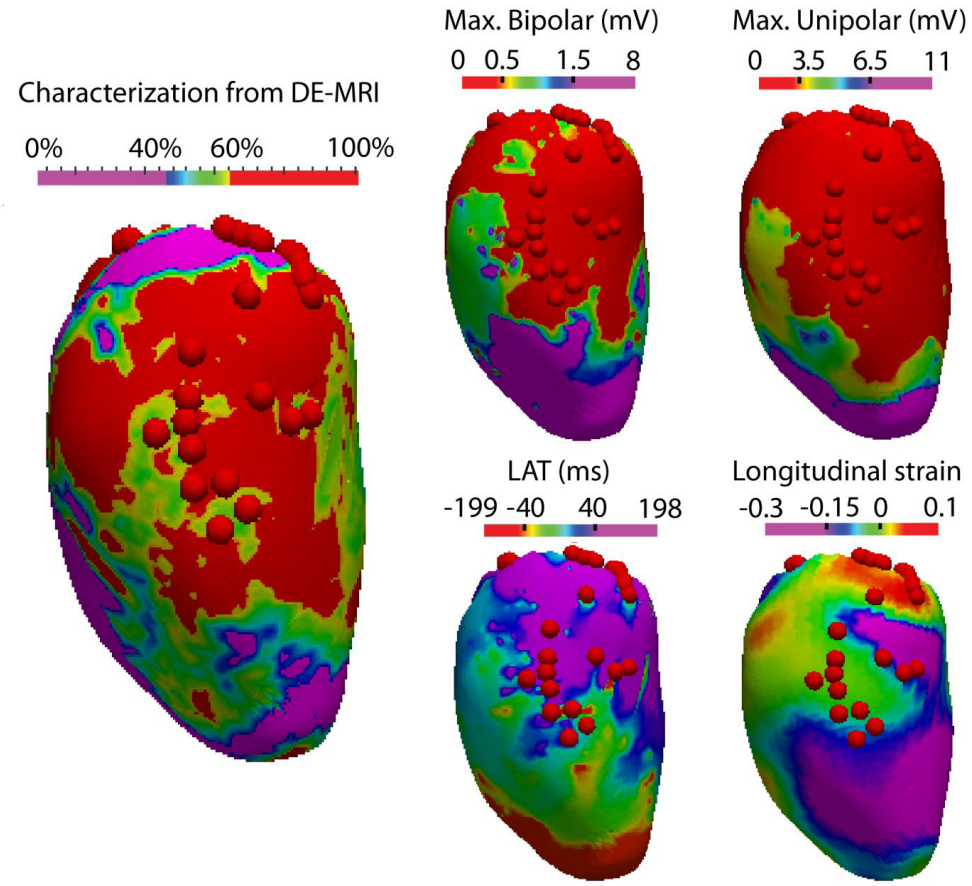

FIGURE 4. **Information integrated by the framework for a 75-year-old man with VT associated with IC. In the scar characterization from DE-MRI, red color represents scar core, purple represents healthy tissue and the rest of the colors represent border zones according to the signal intensity maps. The electrical information is represented by the bipolar voltage map, the unipolar voltage map and the local activation time map. Longitudinal strain calculated at end systole is shown, where negative values represent contraction and positive values indicate stretching. End-systolic strain values are represented on the endocardium at end-diastolic phase to improve visual comparison with the other results. Red spheres represent the ablation targets identified pre-operatively from DE-MRI.**

area and the mitral annulus [37], or (ii) late potential channels. The latter were defined as regions with 2 or more consecutive endocardial electrograms presenting delayed components, localized in the scar area and connecting with healthy tissue, which are not possible to visualize using voltage thresholds [38].

IV. RESULTS

Results from three patients are presented to illustrate the framework's utility for catheter ablation planning and treatment. For these three cases, the left ventricle was segmented from DE-MRI prior to the catheter ablation intervention using the cardiac segmentation module. Then, the module for image-based scar characterization was used to classify the scar core, border zone and healthy myocardium.

The meshes obtained pre-operatively were used during the intervention to guide the procedure. The electro-anatomical maps obtained were then imported into the module for electrical and mechanical characterization from EAM data. Finally, electrical values were projected into the endocardial mesh and ventricular motion was reconstructed.

For each patient, a figure including different measurements obtained by integrating data with the presented framework is shown: segmentation of the left ventricle and scar characterization from DE-MRI, maximum unipolar voltage, maximum bipolar voltage, local activation time recorded with Carto and projected onto the ventricle shape, and longitudinal strain estimated at end systole as presented in [22]. In addition, a comparison between the extension of the scar identified pre-operatively from DE-MRI and intra-operatively using the bipolar maps was also performed.

A. CASE 1

The first patient analyzed for this study was a 75 year old man with VT associated with IC. Fig. 4 shows the results for this patient. In this case, a scar was identified pre-operatively from DE-MRI in the inferior wall of the left ventricle. Three areas were identified as conducting channels

IEEE Journal of Translational Engineering in Health and Medicine

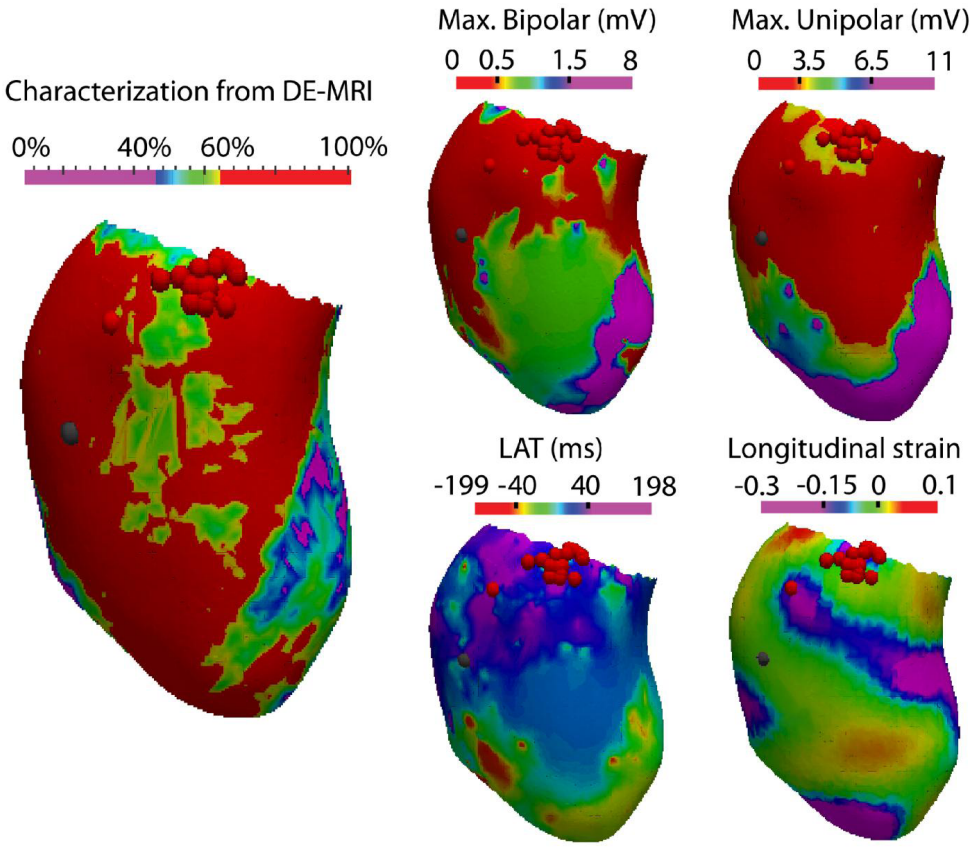

FIGURE 5. **Information integrated by the framework for a 69-year-old man with VT associated to IC. In the scar characterization from DE-MRI, red color represents scar core, purple represents healthy tissue and the rest of the colors represent border zone according to the signal intensity maps. The electrical information is represented by the bipolar voltage map, the unipolar voltage map and the local activation time map. Longitudinal strain calculated at end systole is shown, where negative values represent contraction and positive values indicate stretching. End-systolic strain values are represented on the endocardium at end-diastolic phase to improve visual comparison with the other results. Red spheres represent the ablation targets identified pre-operatively from DE-MRI, while grey speheres represent the ones identified intra-operatively using the electrical maps.**

and, hence, possible ablation targets. After the electrophysiology study, the maximum bipolar voltage showed a very homogeneous scar in comparison with the scar shape obtained from DE-MRI. The scar area defined using the bipolar voltage map was 39% larger compared to the scar identified from DE-MRI, while the border zone area was 11% smaller.

The maximum unipolar voltage map showed a shape and extension of the scar very similar to the one from the maximum bipolar map. The local activation time showed a conduction delay in the areas around the dense scar, where electrical impulse was still propagated. As expected, spatially heterogeneous strain patterns were obtained. In particular, the longitudinal strain showed no contraction or stretching in the dense scar area while it reflected contraction in the surrounding areas.

Ablation was performed at the entrance of each one of the conducting channels identified pre-operatively from DE-MRI, resulting in a non-inducible arrhythmia and hence, a successful intervention.

B. CASE 2

The results for another patient (male, aged 69, VT with IC) are shown in Fig. 5. The DE-MRI study showed an infero-septal scar with a wide longitudinal line of border zone tissue. The bipolar map showed low voltages for the whole scar. The extension of the scar identified with the bipolar map was 23% larger than the one identified from DE-MRI. In this case, the bipolar map showed low voltage values for the whole base of the ventricle, while the scar defined from DE-MRI was only localized in the inferior wall. The border zone area from the bipolar map was 65% larger compared to results from DE-MRI, finding reduced voltage values in a large area of the ventricle.

The unipolar map showed low voltages for the whole scar, being higher at the entrance of the line of border zone tissue identified from DE-MRI. The local activation time presented some heterogeneities at the entrance of this border zone line, as in the case of the unipolar voltage map. The longitudinal strain showed reduced contraction in the inferior wall, with

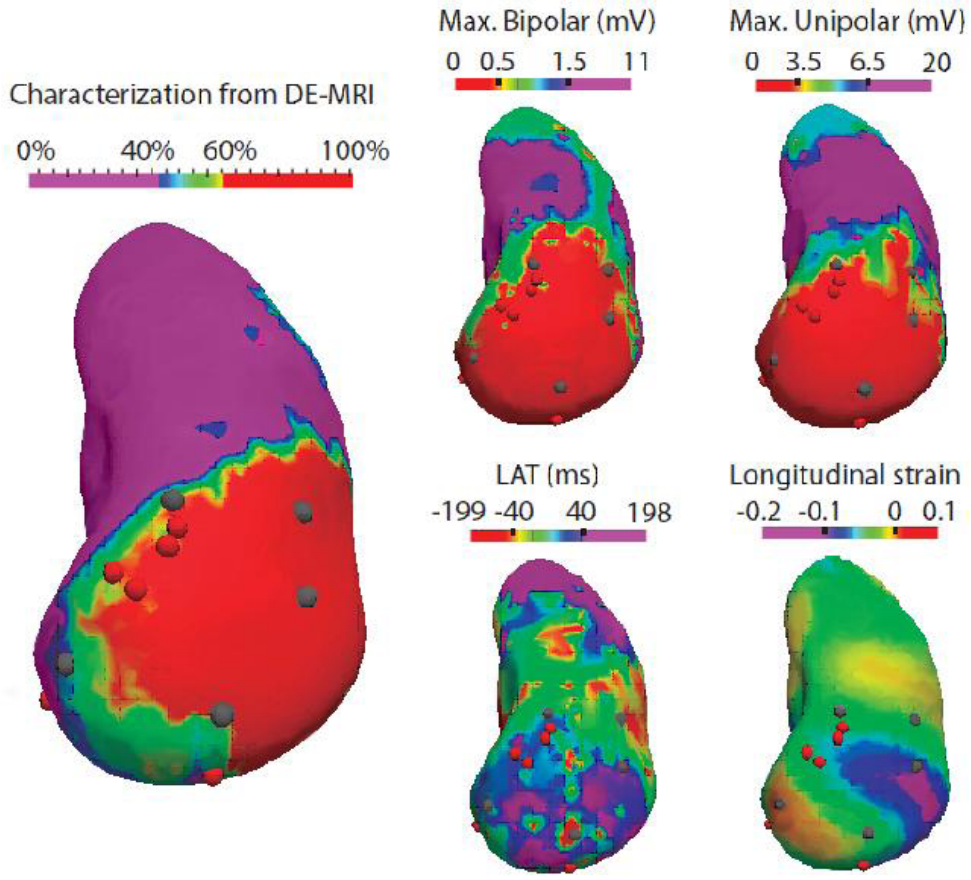

FIGURE 6. **Information integrated by the framework for a 82-year-old man with VT associated to IC. In the scar characterization from DE-MRI, red color represents scar core, purple represents healthy tissue and the rest of the colors represent border zone according to the signal intensity maps. The electrical information is represented by the bipolar voltage map, the unipolar voltage map and the local activation time map. Longitudinal strain calculated at end systole is shown, where negative values represent contraction and positive values indicate stretching. End-systolic strain values are represented on the endocardium at end-diastolic phase to improve visual comparison with the other results. Red spheres represent the ablation targets identified pre-operatively from DE-MRI, while grey speheres represent the ones identified intra-operatively using the electrical maps.**

higher contraction at the entrance of the border zone channel identified from DE-MRI. It is also possible to observe the presence of stretching areas in the dense scar area.

The points of ablation were situated at the entrance of the corridor of border zone that was identified from both DE-MRI and the electrical maps.

C. CASE 3

Fig. 6 shows the results for the third patient (male, aged 82, VT with IC). The DE-MRI study allowed the identification of a scar in the anterior wall. The bipolar map showed a dense scar area 57% larger than the area identified from DE-MRI. On the other hand, the area of border zone tissue was 33% smaller compared to the results DE-MRI.

The unipolar map showed very homogeneous low voltage values for the whole scar. On the other hand, the local activation time showed very heterogeneous patterns. The longitudinal strain was reduced in the whole wall, showing some stretching in the apex.

In this case, ablation was performed at the border zone channels identified from DE-MRI and the local activation time map, as seen from Fig. 6.

V. DISCUSSION

Three study cases were presented, showing multimodal myocardial tissue characterization based on different information sources. Results demonstrated the clinical feasibility of the approach and showed that there is a relation between the shape and extension of the scar identified from the different sources. However, as expected [25], there are also variations between the results from the different modalities. In the three cases presented, the extension of the dense scar area identified using electrical maps was larger than the dense scar area identified from DE-MRI (range 23%–57%). It was possible to identify most of the conducting channels prior to the intervention from DE-MRI, although the electrical maps were necessary to find all of them, as it can be observed from Fig. 4–6.

IEEE Journal of Translational Engineering in Health and Medicine

Maximum bipolar and unipolar voltage maps showed a similar shape and extension of the scar. In the case of the second patient, the unipolar voltage map showed areas with low voltage values that were not identified by the bipolar voltage map. These differences could be explained because endocardial bipolar maps give information about subendocardial activation, while endocardial unipolar voltage maps give transmural information [39].

The local activation time map was able to detect the conducting channels for the three patients presented, showing delayed activation in comparison to the healthy myocardium. Unipolar and bipolar maps were not able to distinguish all conducting channels, showing a homogeneous scar core. Activation maps during sinus rhythm have been recently proposed to better define the areas of interest during substrate mapping as areas with ventricular activation after the QRS [38], [40].

The resulting longitudinal strain presented heterogeneous spatial patterns. For the cases analyzed, stretching areas at end systole were found in the scar core, with contraction around these areas. Heterogeneities in the scar areas could be explained by the tethering to adjacent tissue [41], being the contraction or stretching due to passive motion. Moreover, the presence of scar tissue affects the motion of the whole ventricle and thereby its deformation.

The example cases presented showed that the proposed framework is feasible and potentially useful for the analysis and integration of multi-modal information for scar characterization. It could be used intra-operatively for guidance and monitoring of therapy by integrating it with any EAM system.

The results obtained show the feasibility of the technique in a clinical setting. They do not constitute, however, a detailed quantitative validation on the clinical impact of this technique (*e.g.* in terms of reduction of interventional time or X-ray radiation dose). A prospective study of clinical impact that includes a randomized population of subjects suffering from VT and undergoing radiofrequency ablation using this technique and the standard-of-practice is the natural next step. This work does, however, offer, as a first step, the preliminary proof-of-concept evidence for such a study.

Furthermore, the presented framework also allows annotating both the electrical signals and the visualized meshes. In addition, all the information used can be exported for subsequent analysis or for research purposes.

One limitation of this framework is that motion and deformation were only estimated for the endocardium of the left ventricle. The reason is that the spatiotemporal atlas used only includes shape and motion information about the endocardium of the left ventricle. Extension to other cavities could be considered for future work. Moreover, this framework could be extended in multiple ways (including algorithms for predictive analysis, automatic detection of conducting channels. . .)

VI. CONCLUSION

A framework for the integrated analysis of DE-MRI, electrical and mechanical information has been presented. Integrating multi-modal information can be helpful for interventional guidance and monitoring of radiofrequency ablation procedures where myocardial scar tissue characterization is required. The three presented example cases show that the relevance of the information extracted from the different sources can vary depending on the patient analyzed (*i.e.* conducting channels that are visible in DE-MRI but not in the bipolar and unipolar maps and vice versa). The framework can also be helpful for research purposes, facilitating the study of the relation between electrical and mechanical properties of the tissue, as well as the information obtained from DE-MRI.

ACKNOWLEDGMENT

The authors would like to thank the people involved in the development of GIMIAS and the implementation of the segmentation module: V. Barbarito, C. Butakoff, L. Carotenuto, C. Hoogendoorn, X. Planes, C. Riccobene, C. Tobon-Gomez, F. M. Sukno, and L. Serra.

REFERENCES

[1] J. M. Miller and D. P. Zipes, "Catheter ablation of arrhythmias," *Circulation*, vol. 106, pp. e203–e205, Dec. 2002.
[2] W. G. Stevenson, "Ventricular scars and ventricular tachycardia," *Trans. Amer. Clin. Climatol. Assoc.*, vol. 120, pp. 403–412, 2009.
[3] R. J. Kim *et al.*, "Relationship of MRI delayed contrast enhancement to irreversible injury, infarct age, and contractile function," *Circulation*, vol. 100, no. 19, pp. 1992–2002, Nov. 1999.
[4] E. Wu, R. M. Judd, J. D. Vargas, F. J. Klocke, R. O. Bonow, and R. J. Kim, "Visualisation of presence, location, and transmural extent of healed Q-wave and non-Q-wave myocardial infarction," *Lancet*, vol. 357, no. 9249, pp. 21–28, Jan. 2001.
[5] A. T. Yan *et al.*, "Characterization of the peri-infarct zone by contrast-enhanced cardiac magnetic resonance imaging is a powerful predictor of post-myocardial infarction mortality," *Circulation*, vol. 114, no. 1, pp. 32–39, Jul. 2006.
[6] A. Codreanu *et al.*, "Electroanatomic characterization of post-infarct scars comparison with 3-dimensional myocardial scar reconstruction based on magnetic resonance imaging," *J. Amer. College Cardiol.*, vol. 52, no. 10, pp. 839–842, 2008.
[7] D. Andreu *et al.*, "Integration of 3D electroanatomic maps and magnetic resonance scar characterization into the navigation system to guide ventricular tachycardia ablation," *Circulat. Arrhythm Electrophysiol.*, vol. 4, no. 5, pp. 674–683, Oct. 2011.
[8] J. Fernandez-Armenta *et al.*, "Three-dimensional architecture of scar and conducting channels based on high resolution ce-CMR: Insights for ventricular tachycardia ablation," *Circulat. Arrhythm Electrophysiol.*, vol. 6, no. 3, pp. 528–537, Jun. 2013.
[9] B. Desjardins *et al.*, "Infarct architecture and characteristics on delayed enhanced magnetic resonance imaging and electroanatomic mapping in patients with postinfarction ventricular arrhythmia," *Heart Rhythm*, vol. 6, no. 5, pp. 644–651, May 2009.
[10] S. Gupta *et al.*, "Delayed-enhanced MR scar imaging and intraprocedural registration into an electroanatomical mapping system in post-infarction patients," *JACC Cardiovascular Imag.*, vol. 5, no. 2, pp. 207–210, 2012.
[11] E. Perez-David *et al.*, "Noninvasive identification of ventricular tachycardia-related conducting channels using contrast-enhanced magnetic resonance imaging in patients with chronic myocardial infarction: Comparison of signal intensity scar mapping and endocardial voltage mapping.," *J. Amer. College Cardiol.*, vol. 57, no. 2, pp. 184–194, Jan. 2011.

[12] E. Dikici, T. O'Donnell, R. Setser, and R. D. White, "Quantification of delayed enhancement MR images," in *Medical Image Computing and Computer-Assisted Intervention*, vol. 3216. Berlin, Germany: Springer-Verlag, 2004, pp. 250–257.
[13] R. Berbari, N. Kachenoura, F. Frouin, A. Herment, E. Mousseaux, and I. Bloch, "An automated quantification of the transmural myocardial infarct extent using cardiac DE-MR images," in *Proc. Annu. Int. Conf. IEEE Eng. Med. Biol. Soc.*, vol. 2009. Sep. 2009, pp. 4403–4406.
[14] X. Alba, R. M. Figueras i Ventura, K. Lekadir, and A. F. Frangi, "Conical deformable model for myocardial segmentation in late-enhanced MRI," in *Proc. 9th IEEE ISBI*, May 2012, pp. 270–273.
[15] E. Heiberg, H. Engblom, J. Engvall, E. Hedström, M. Ugander, and H. Arheden, "Semi-automatic quantification of myocardial infarction from delayed contrast enhanced magnetic resonance imaging," *Scandinavian Cardiovascular J.*, vol. 39, no. 5, pp. 267–275, Oct. 2005.
[16] Q. Tao *et al.*, "Automated segmentation of myocardial scar in late enhancement MRI using combined intensity and spatial information," *Magn. Reson. Med.*, vol. 64, no. 2, pp. 586–594, Aug. 2010.
[17] X. Alba, R. M. Figueras i Ventura, K. Lekadir, and A. F. Frangi, "Healthy and scar myocardial tissue classification in DE-MRI," in *Statistical Atlases and Computational Models of the Heart, Imaging and Modelling Challenges*, vol. 7746. Berlin, Germany: Springer-Verlag, 2013, pp. 62–70.
[18] V. Positano *et al.*, "A fast and effective method to assess myocardial necrosis by means of contrast magnetic resonance imaging," *J. Cardiovascular Magn. Reson.*, vol. 7, no. 2, pp. 487–494, 2005.
[19] T. P. O'Donnell, N. Xu, R. M. Setser, and R. D. White, "Semi-automatic segmentation of nonviable cardiac tissue using cine and delayed enhancement magnetic resonance images," *Proc. SPIE*, vol. 5031, pp. 242–251, May 2003.
[20] H. E. Botker *et al.*, "Electromechanical mapping for detection of myocardial viability in patients with ischemic cardiomyopathy," *Circulation*, vol. 103, no. 12, pp. 1631–1637, Mar. 2001.
[21] P. J. Psaltis and S. G. Worthley, "Endoventricular electromechanical mapping-the diagnostic and therapeutic utility of the NOGA XP cardiac navigation system," *J. Cardiovascular Transl. Res.*, vol. 2, no. 1, pp. 48–62, Mar. 2009.
[22] A. R. Porras *et al.*, "Interventional endocardial motion estimation from electroanatomical mapping data: Application to scar characterization," *IEEE Trans. Biomed. Eng.*, vol. 60, no. 5, pp. 1217–1224, May 2013.
[23] J. Lessick, G. Hayam, A. Zaretsky, S. A. Reisner, Y. Schwartz, and S. A. Ben-Haim, "Evaluation of inotropic changes in ventricular function by NOGA mapping: Comparison with echocardiography," *J. Appl. Physiol.*, vol. 93, no. 2, pp. 418–426, Aug. 2002.
[24] H. U. Klemm *et al.*, "Simultaneous mapping of activation and motion timing in the healthy and chronically ischemic heart," *Heart Rhythm*, vol. 3, no. 7, pp. 781–788, Jul. 2006.
[25] J. A. Fallavollita, U. Valeti, S. Oza, and J. M. Canty, Jr., "Spatial heterogeneity of endocardial voltage amplitude in viable, chronically dysfunctional myocardium," *Basic Res. Cardiol.*, vol. 99, no. 3, pp. 212–222, May 2004.
[26] R. Kornowski *et al.*, "Preliminary animal and clinical experiences using an electromechanical endocardial mapping procedure to distinguish infarcted from healthy myocardium," *Circulation*, vol. 98, no. 11, pp. 1116–1124, 1998.
[27] I. Larrabide *et al.*, "GIMIAS: An open source framework for efficient development of research tools and clinical prototypes," in *Functional Imaging and Modeling of the Heart*, vol. 5528. Berlin, Germany: Springer-Verlag, 2009, pp. 417–426.
[28] S. Ordas, E. Oubel, R. Leta, F. Carreras, and A. F. Frangi, "A statistical shape model of the heart and its application to model-based segmentation," *Proc. SPIE*, vol. 6511, p. 65111K, Mar. 2007.
[29] C. Hoogendoorn *et al.*, "A high-resolution atlas and statistical model of the human heart from multislice CT," *IEEE Trans. Med. Imag.*, vol. 32, no. 1, pp. 28–44, Jan. 2013.
[30] C. Tobon-Gomez, C. Butakoff, S. Aguade, F. Sukno, G. Moragas, and A. F. Frangi, "Automatic construction of 3D-ASM intensity models by simulating image acquisition: Application to myocardial gated SPECT studies," *IEEE Trans. Med. Imag.*, vol. 27, no. 11, pp. 1655–1667, Nov. 2008.
[31] C. Butakoff, S. Balocco, F.M. Sukno, C. Hoogendoorn, C. Tobon-Gomez, G. Avegliano and A.F. Frangi, "Left-ventricular epi- and endocardium extraction from 3D ultrasound images using an automatically constructed 3D ASM," *Comput. Methods Biomech. Biomed. Eng., Imag. Vis.*, to be published.
[32] C. Tobon-Gomez, F. M. Sukno, C. Butakoff, M. Huguet, and A. F. Frangi, "Automatic training and reliability estimation for 3D ASM applied to cardiac MRI segmentation," *Phys. Med. Biol.*, vol. 57, no. 13, pp. 4155–4174, Jul. 2012.
[33] H. C. van Assen *et al.*, "SPASM: A 3D-ASM for segmentation of sparse and arbitrarily oriented cardiac MRI data," *Med. Imag. Anal.*, vol. 10, no. 2, pp. 286–303, Apr. 2006.
[34] P. J. Besl and N. D. McKay, "A method for registration of 3-D shapes," *IEEE Trans. Pattern Anal. Mach. Intell.*, vol. 14, no. 2, pp. 239–256, Feb. 1992.
[35] M. D. Cerqueira *et al.*, "Standardized myocardial segmentation and nomenclature for tomographic imaging of the heart. A statement for healthcare professionals from the cardiac imaging committee of the council on clinical cardiology of the american heart association," *Circulation*, vol. 105, no. 4, pp. 539–542, 2002.
[36] K. U. Bauner *et al.*, "Assessment of myocardial viability with 3D MRI at 3 T," *AJR Amer. J. Roentgenol.*, vol. 192, no. 6, pp. 1645–1650, Jun. 2009.
[37] A. Arenal *et al.*, "Tachycardia-related channel in the scar tissue in patients with sustained monomorphic ventricular tachycardias: Influence of the voltage scar definition," *Circulation*, vol. 110, no. 17, pp. 2568–2574, Oct. 2004.
[38] A. Berruezo *et al.*, "Combined endocardial and epicardial catheter ablation in arrhythmogenic right ventricular dysplasia incorporating scar dechanneling technique," *Circulat. Arrhythmia Electrophysiol.*, vol. 5, no. 1, pp. 111–121, Feb. 2012.
[39] M. D. Hutchinson *et al.*, "Endocardial unipolar voltage mapping to detect epicardial ventricular tachycardia substrate in patients with nonischemic left ventricular cardiomyopathy," *Circulat. Arrhythmia Electrophysiol.*, vol. 4, no. 1, pp. 49–55, 2011.
[40] P. Vergara *et al.*, "Late potentials abolition as an additional technique for reduction of arrhythmia recurrence in scar related ventricular tachycardia ablation," *J. Cardiovascular Electrophysiol.*, vol. 23, no. 6, pp. 621–627, 2012.
[41] J. Gorcsan, "Echocardiographic strain imaging for myocardial viability: An improvement over visual assessment?" *Circulation*, vol. 112, no. 25, pp. 3820–3822, 2005.

ANTONIO R. PORRAS received the B.Sc. degree in computer systems and the B.Sc. degree in computational engineering from the Universidad de Córdoba, Córdoba, Spain, in 2006 and 2008, respectively, and the M.Sc. degree in biomedical engineering from the Universitat de Barcelona, Barcelona, Spain, and the Universitat Politècnica de Catalunya, Barcelona, in 2010. He was also a Visiting Student with the Chalmers University of Technology, Gothenburg, Sweden. He is currently pursuing the Ph.D. degree with Universitat Pompeu Fabra, Barcelona. His main research interest is biomedical data/images integration for motion and deformation estimation of the heart.

GEMMA PIELLA received the B.Sc. degree in telecommunication engineering from the Universitat Politècnica de Catalunya (UPC), Barcelona, Spain, in 1999, and the Ph.D. degree from the University of Amsterdam, Amsterdam, The Netherlands, in 2003. From 2003 to 2004, she was with UPC as a Visiting Professor. She was with the École Nationale des Tèlècommunications, Paris, France, as a Marie Curie Post-Doctoral Fellow. Since 2005, she has been with the Department of Technology, Universitat Pompeu Fabra, Barcelona. She was a recipient of the Ramón y Cajal Research Fellowship from 2007 to 2011. Her work has focused on multiresolution analyses, adaptive wavelets, geometrical image processing, and image fusion and registration.

IEEE Journal of Translational Engineering in Health and Medicine

ANTONIO BERRUEZO was qualified in Medicine and Surgery at the Universidad de Granada, Granada, Spain, in 1993, and received the Cardiology title in 2002. He completed the two-years fellowship program of the Hospital Clínic de Barcelona, and received the Ph.D. degree from the Universitat de Barcelona, Barcelona, Spain, in 2009. He is currently an Associate Professor with the Universitat de Barcelona. He has been awarded with the European Accreditation in Interventional Cardiac Electrophysiology. Since 2005, he has been with the Arrhytmia Section, Thorax Institute of Hospital Clínic de Barcelona, Universitat de Barcelona. He is involved in several research projects related with atrial fibrillation, cardiac resynchronization therapy, and ventricular arrhythmias, and being ventricular tachycardia ablation is his main area of interest. He has authored over 100 papers related to cardiac electrophysiology in peer-reviewed journals.

JUAN FERNÁNDEZ-ARMENTA received the degree in medicine from the Universidad de Seville, Seville, Spain, in 2003, and the Cardiology Residency Program at Hospital Universitario Virgen Macarena and Valme. He has conducted the Cardiac Electrophisiology Fellowship Program of the Hospital Clínic de Barcelona. He received the Ph.D. degree from the Universitat de Barcelona, Barcelona, Spain, in 2014. He has been awarded with the European Accreditation in Interventional Cardiac Electrophysiology and Cardiac Pacing. His main research fields are ventricular arrhythmias and sudden cardiac death.

ALEJANDRO F. FRANGI (S'95–M'01–SM'05–F'14) received the bachelor's degree in telecommunications engineering from the Universitat Politècnica de Catalunya, Barcelona, Spain, in 1996. He was a Ramón y Cajal Research Fellow with the Universidad de Zaragoza, Zaragoza, Spain (2003–2004), and Universitat Pompeu Fabra (UPF), Barcelona (2004–2007), and an Associate Professor at UPF (2007–2012). He is currently a Professor of Biomedical Image Computing with the University of Sheffield, Sheffield, U.K. He has authored over 130 peer-reviewed journal papers. His main research interests are in medical image computing, medical imaging, and image-based computational physiology. He has been awarded the IEEE EMBS Early Career Award (2006), the ICREA Academia Prize (2009), and the UPF Medal (2011). He is the Director of the Centre for Computational Imaging and Simulation Technologies in Biomedicine, and has provided the scientific leadership and funding raising effort to develop the GIMIAS open-source platform for rapid prototyping to ease precommercial clinical uptake of the software prototypes developed within CISTIB.